ACS APPLIED MATERIALS & INTERFACES

Research Article

www.acsami.org

Development of Both Methotrexate and Mitomycin C Loaded PEGylated Chitosan Nanoparticles for Targeted Drug Codelivery and Synergistic Anticancer Effect

Mengmeng Jia,[†,⊥] Yang Li,[†,§,⊥] Xiangrui Yang,[†] Yuancan Huang,[†] Hongjie Wu,[∥] Yu Huang,[†] Jinyan Lin,[†,§] Yanxiu Li,[†,∥] Zhenqing Hou,*[,†] and Qiqing Zhang*[,‡]

[†]Research Center of Biochemical Engineering & Department of Biomaterials, College of Materials, [§]Department of Chemistry, College of Chemistry & Chemical Engineering, [∥]School of Pharmaceutical Science, Xiamen University, Xiamen 361005, Fujian, China

[‡]Institute of Biomedical Engineering, Chinese Academy of Medical Science & Peking Union Medical College, Tianjin 300192, China

Supporting Information

ABSTRACT: Codelivery of multiple drugs with one kind of drug carriers provided a promising strategy to suppress the drug resistance and achieve the synergistic therapeutic effect in cancer treatment. In this paper, we successfully developed both methotrexate (MTX) and mitomycin C (MMC) loaded PEGylated chitosan nanoparticles (CS-NPs) as drug delivery systems, in which MTX, as a folic acid analogue, was also employed as a tumor-targeting ligand. The new drug delivery systems can coordinate the early phase targeting effect with the late-phase anticancer effect. The (MTX+MMC)-PEG-CS-NPs possessed nanoscaled particle size, narrow particle size distribution, and appropriate multiple drug loading content and simultaneously sustained drug release. In vitro cell viability tests indicated that the (MTX+MMC)-PEG-CS-NPs exhibited concentration- and time-dependent cytotoxicity. Moreover, in vitro cellular uptake suggested that the (MTX+MMC)-PEG-CS-NPs could be efficiently taken up by cancer cells by FA receptor-mediated endocytosis. On the other hand, the (MTX+MMC)-PEG-CS-NPs can codelivery MTX and MMC to not only achieve the high accumulation at the tumor site but also more efficiently suppress the tumor cells growth than the delivery of either drug alone, indicating a synergistic effect. In fact, the codelivery of two anticancer drugs with distinct functions and different anticancer mechanisms was key to opening the door to their targeted drug delivery and synergistic anticancer effect. Therefore, the (MTX+MMC)-PEG-CS-NPs as targeted drug codelivery systems might have important potential in clinical implications for combination cancer chemotherapy.

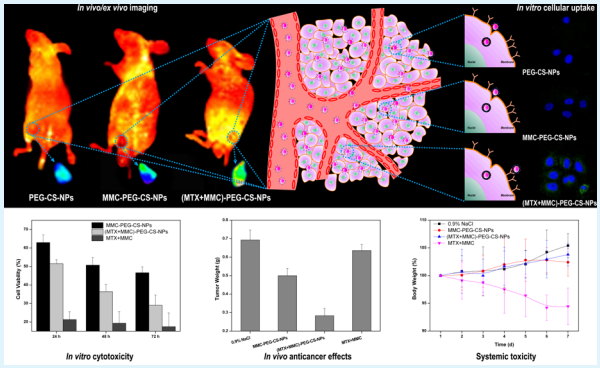

KEYWORDS: *methotrexate, mitomycin C, PEGylated chitosan, drug delivery, receptor-mediated targeting*

INTRODUCTION

Existing chemotherapy is conceived as one of the primary options to treat cancer, which is also a leading cause of death worldwide.[1] However, there still exist some intractable problems. For example, the undesirable side effects, low bioavailability, or development of drug resistance limited its application. Even worse, it was difficult to remove tumor tissue completely in most cases.[2]

To overcome these drawbacks, nanoscaled drug delivery systems (NDDS) have been regarded as one of the most promising approaches to deal with cancer via the enhanced permeation and retention (EPR) effect.[3] Over the past few decades, various NDDS including liposomes, polymeric NPs, inorganic NPs, micelles, dendrimers, and carbon nanotubes have attracted a lot of attention for drug delivery, and these studies have demonstrated these NDDS can significantly improve the therapeutic efficiency of various chemotherapeutic drugs while reducing their toxicity.[4,5]

Another promising application of NDDS may be the codelivery of different drugs.[6−8] Synergistic codelivery of multiple drugs, with combined pharmacological activities originating from different physicochemical characteristics, provided a promising strategy to overcome serious toxicity and other side effects that limited the potential exploitation of a series of chemotherapeutic drugs by countering biological compensation, accessing site-specific multiple-target mechanisms.[9−11] Compared to delivering a single drug, delivering multiple drugs simultaneously to the same tumor cells *in vitro* and *in vivo*, which could damage or kill tumor cells at different

Received: April 2, 2014
Accepted: June 30, 2014
Published: June 30, 2014

Scheme 1. Illustrations of the Preparation (A), Targeted Delivery to Tumor Cells and Simultaneous Multiple Drug Delivery of the (MTX+MMC)-PEG-CS-NPs (B)

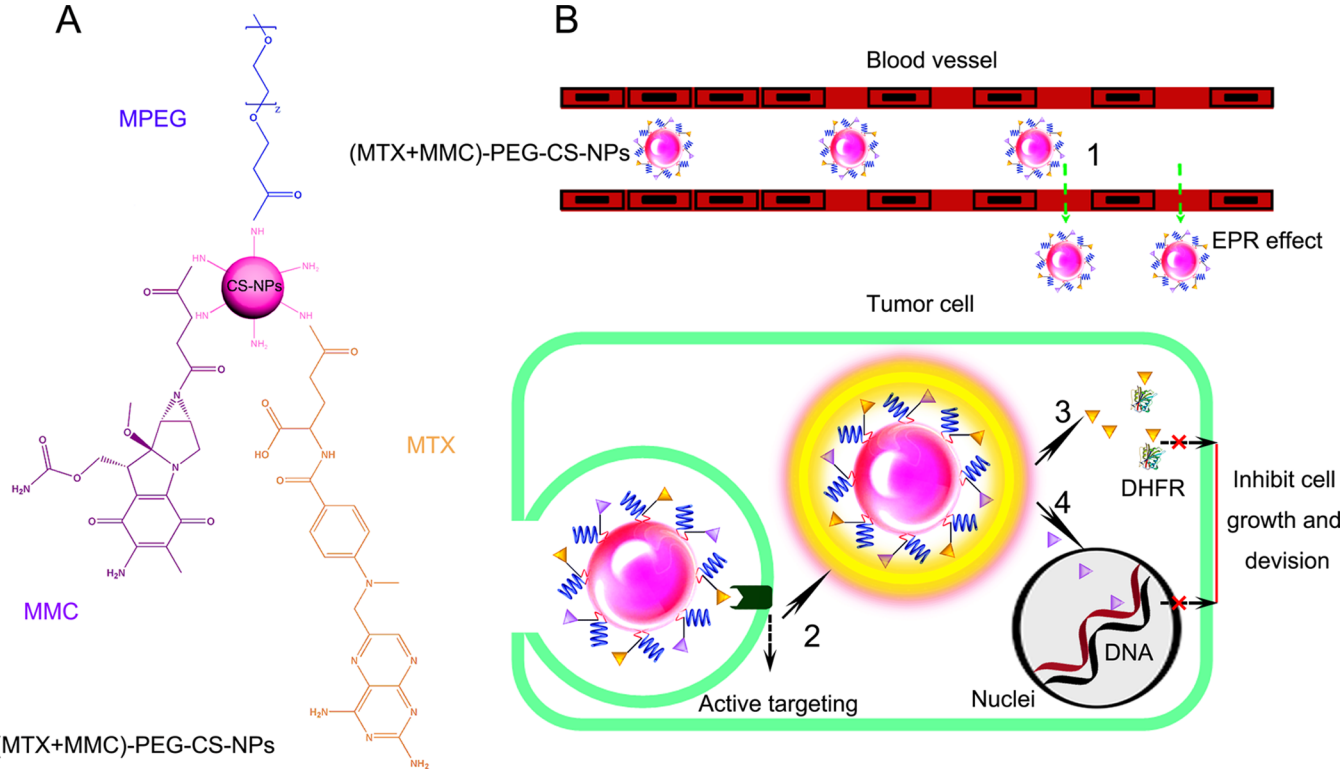

stages of their growth cycles through distinct mechanisms of action, have been proposed to suppress the drug resistance and achieve the synergistic therapeutic effect in cancer treatment.[12,13] Recently, a series of NDDS including liposomes, polymeric NPs, and micelles have been designed for codelivery of different chemotherapeutic drugs.[14−19] Although many works have been made on a single carrier for two or more chemotherapeutic drugs,[8,14−19] codelivery of multiple anticancer drugs with one of them possessing a Janus role has not been reported before.

MMC and MTX were among the most widely used anticancer drugs in cancer chemotherapy, due to their potential anticancer efficiency against various tumors.[20,21] They, however, are drugs with distinct physicochemical characteristics and different anticancer mechanisms.[22−25] On the one hand, MMC, as a bioreductively activated agent, could be transported into the nuclei and reacted with DNA to inhibit DNA synthesis and nuclear division.[26] On the other hand, MTX, as an antimetabolite and antifolate drug, could be delivered to the cytoplasm and reacted with dihydrofolate reductase (DHFR) to inhibit the metabolism of folic acid (FA), leading to a block in nucleic acid biosynthesis.[27] A clinical study has shown that combination chemotherapy with MMC and MTX was potential for metastatic breast cancer pretreated with anthracycline and taxanes.[28] Moreover, owing to the structural similarity, MTX can enter cells through similar transport systems (reduced folate carrier, proton-coupled FA transporter, and membrane-associated FA receptor) as FA.[29−33] These encouraged the vision of Janus-like MTX acting as an early phase targeting ligand coordinated with a late-phase anticancer drug with promising potential. Particularly, the Janus role has attracted an increasing interest and may provide a new concept in scientific research.[34−36]

As the key point for successful combination therapy, a straightforward solution is to design simple codelivery systems to unify the pharmacokinetics and cellular uptake of multiple drugs. The systems based on CS polymer are successful examples. The polymer presented great advantages such as biocompatibility, biodegradability, low toxicity and immunogenicity, and easy surface functionalization of some small molecules and has been extensively investigated in drug, protein, and gene delivery.[37−40] Previously, we synthesized the CS-NPs by the combination of ionic gelation and chemical cross-linking method and prepared the MMC-loaded PEGylated CS-NPs.[41] We also prepared the MTX-loaded PEGylated CS-NPs.[42] Remarkable improvements have been confirmed in the therapeutic effects. The results also inspired our motivation of adopting the CS-NPs as drug carriers for codelivery of multiple anticancer drugs.

In this paper, we used the CS-NPs as drug carriers, followed by the PEGylation with MPEG-SPA. To avoid the premature drug leakage and burst release during blood circulation and increase the therapeutic efficiency, the multiple anticancer drugs (MMC and MTX) were chemically conjugated to PEGylated CS-NPs to obtain the (MTX+MMC)-PEG-CS-NPs (Scheme 1). Loading drug within the NPs by chemical conjugation was preferred over physical adsorption, which could be of utmost importance for drug delivery, especially in vivo. The integrated NPs are based on the following structure: (i) an inner core, which was CS-NPs to load the multiple drugs with high loading efficiency, (ii) an outer shell, which was MPEG to increase the stability, reduce protein adsorption and recognition by macrophages of the mononuclear phagocyte system, and improve the passive targeting efficiency,[43] and (iii) multiple drugs, which were anticancer drug (MMC) and Janus-like agent (MTX) to potentially exert the synergistic codelivery

effect with a role change: before internalized inside the tumor cells, MMC acted as a prodrug and MTX as a targeting ligand to endow the NPs with the active target activity. Once internalized, MMC functioned as a first drug delivered to the nuclei and MTX as a second one to the cytoplasm.

As proof-of-principle, our study demonstrated that simultaneous delivery of MMC and MTX to solid tumors was feasible in vivo using the PEGylated CS-NPs. The physicochemical characterization of the (MTX+MMC)-PEG-CS-NPs were performed in detail using FTIR, DLS, SLS, SEM, and TEM in addition to in vitro drug release, and their effectiveness was tested in vitro in HeLa cells and in vivo in H_{22} tumor-bearing mice.

EXPERIMENTAL SECTION

Materials. All chemical reagents were of analytical grade and used without further purification unless otherwise stated. Chitosan (CS, Mw = 70,000 Da, 95% degree of deacetylation) was purchased from Zhejiang Aoxing Biotechnology Co., Ltd. (Zhengjiang, China). 1-Ethyl-3-(3-(dimethylamino)propyl) carbodiimide (EDC), *N*-hydroxysuccinimide (NHS), and crude proteases from bovine pancreas (Type I, ⩾5 units/mg solid) were purchased from Sigma Chemical Corp (St. Louis, MO, USA). Folate (FA) and methotrexate (MTX) were purchased from Bio Basic Inc. (Markham, Ontario, Canada). *N*-Succinimidyl ester of methoxypolyethylene glycol propionic acid (MPEG-SPA, Mw = 2,000 Da) was purchased from Jiaxing Biomatrix Inc. (Zhengjiang, China). Mitomycin C (MMC, purity grade = 99.5%) was purchased from Hisun Pharmaceutical Co., Ltd. (Zhengjiang, China). A dialysis bag (Mw = 8,000 to 14,000 Da) was ordered from Greenbird Inc. (Shanghai, China). Deionized water (DI water) was used throughout. Fetal bovine serum (FBS) was purchased from Gibco Life Technologies (AG, Switzerland). 0.25% Trypsin-EDTA and penicillin-streptomycin solution was from Invitrogen. Dulbecco's Modified Eagle's Medium (DMEM) was from Sigma-Aldrich. All solvents used in this study were HPLC grade. HeLa cells were provided by American Type Culture Collection (ATCC).

Preparation of (MTX+MMC)-PEG-CS-NPs. The CS-NPs were prepared by ionic gelation combined with a chemical cross-linking method according to our recently reported procedure with minor differences.[35] MPEG-SPA (150 mg) was added into the CS-NPs suspension (25 mL, 6.4 mg/mL) accompanied by vigorous stirring for 4 h. The prepared PEG-CS-NPs were dialyzed against DI water. Succinic anhydride activated MMC (S-MMC, 50 mg)[35] and EDC (260 mg) were added into the PEG-CS-NPs suspension (25 mL, 8.3 mg/mL) by vigorous stirring for 2 h. The prepared MMC-PEG-CS-NPs were dialyzed against DI water. MTX (10 mg), EDC (50 mg), and NHS (5 mg) were added into the MMC-PEG-CS-NPs suspension (25 mL, 2.7 mg/mL). The prepared (MTX+MMC)-PEG-CS-NPs were centrifuged at 20,000 rpm for 30 min at 4 °C, washed with PBS/DI water, and lyophilized for 24 h.

Drug Loading Content. The amount of multiple drugs was assayed using a high-performance liquid chromatography (HPLC, Waters Associates, Milford, MA, USA) system with the following conditions: stationary phase, Symmetry C18 column (250 mm × 4.6 mm, 5 μm); temperature, 25 °C; elution flow rate, 1 mL/min. The mobile phase for the determination of MTX was methanol/PBS (pH 6.0) (40/60, v/v), and that for MMC was methanol/DI water (35/65, v/v). The detection wavelength for the determination of MTX was 306 nm, and that for MMC was 365 nm. The drug-loading content (DLC) was calculated using the equations listed below:[44]

$$\text{DLC (wt\%)} = (\text{weight of loaded drug}/\text{weight of drug} - \text{loaded NPs}) \times 100\%$$

$$\text{while weight of loaded drug} = \text{total weight of drug} - \text{weight of drug in the supernatant}$$

FTIR Analysis. The lyophilized (MTX+MMC)-PEG-CS-NPs were investigated using FTIR (Thermo Scientific, UT, USA) from 3,400 to 600 cm^{-1} at 4 cm^{-1} spectral resolution. The MMC-PEG-CS-NPs and PEG-CS-NPs were used for comparison.

Particle Size, Polydispersity Index (PDI), Zeta Potential, and Morphology. The average particle size and PDI of the (MTX+MMC)-PEG-CS-NPs were performed by DLS using a Malvern Zetasizer Nano-ZS (Malvern Instruments, Worcestershire, UK). The zeta potential of the (MTX+MMC)-PEG-CS-NPs was estimated by ELS with Zetaplus (Brookhaven Instruments Corporation, Holtsville, NY, USA). Particle size was evaluated by intensity distribution. The morphology of the (MTX+MMC)-PEG-CS-NPs was visualized by SEM (LEO 1530VP, Oberkochen, Germany) operating at 20 kV and TEM (JEM 1400, JEOL, Tokyo, Japan) operating at 200 kV. Prior to the analysis, each kind of the samples was diluted in DI water followed by ultrasonic dispersion.

In Vitro Drug Release. The release of MMC from the (MTX+MMC)-PEG-CS-NPs was determined by dialysis technique using a dialysis bag (Mw = 8,000−12,000 Da). The lyophilized NPs were dialyzed against PBS (pH 7.4 or pH 7.4 with crude proteases) at 37 °C. At the predesigned time, 2 mL of the release medium was completely withdrawn and subsequently replaced with the 2 mL of fresh PBS. The release of MMC and MTX was determined by a HPLC method as described above.

Cell Culture. HeLa cells were cultured in FA-deficient DMEM supplemented with 10% fetal bovine serum (FBS) and 1% penicillin-streptomycin. This cell line has a high level of FA receptor expression. The cells were cultivated in a humidified atmosphere containing 5% CO_2 at 37 °C.

In Vitro Cellular Uptake. To facilitate the observation of cellular uptake, fluorescein isothiocyanate (FITC) was conjugated to various PEG-CS-NPs. HeLa cells were seeded at a density of 1×10^5 cells per well in 6-well plates with their specific cell culture medium. The cells were incubated at 37 °C and 5% CO_2 for 24 h. 100 μL of the FITC labeled PEG-CS-NPs, MMC-PEG-CS-NPs, or (MTX+MMC)-PEG-CS-NPs at equivalent FITC concentration was added and incubated further for 12 h. The cells were washed with PBS, fixed with 4% paraformaldehyde, and stained with Hoechst 33258. The cells were observed using a Leica TCS SP5 confocal laser scanning microscopy (CLSM, Leica Microsystems, Mannheim, Germany).

In Vitro Cell Viability Tests. The cytotoxicity of the (MTX+MMC)-PEG-CS-NPs was evaluated by MTT assay. HeLa cells were seeded at a density of 1×10^4 cells per well in 96-well plates, preincubated for 24 h, and then incubated with the (MTX+MMC)-PEG-CS-NPs for 24, 48, or 72 h. The (MTX+MMC)-PEG-CS-NPs with MMC dose ranged from 5 to 80 μg/mL. After 24, 48, or 72 h incubation, the medium was replaced with fresh serum-containing medium. The cells were then carefully washed with PBS, and then MTT was added and incubated for further 2 h. Absorbance at 490 nm was measured using a Bio-Rad Model 680 microplate reader (Richmond, CA, USA). The cells treated with the PEG-CS-NPs, MMC-PEG-CS-NPs, and MTX+MMC were used as controls.

In Vivo/Ex Vivo Tumor Targeting Imaging. Cy5.5 NHS, a near-infrared fluorescent probe, was conjugated to the (MTX+MMC)-PEG-CS-NPs. For in vivo imaging, 0.2 mL of the Cy5.5 NHS labeled (MTX+MMC)-PEG-CS-NPs were injected into mice bearing the H_{22} tumor via lateral tail vein. Imaging was performed at 10, 30 min, 1, 2, 4, and 6 h after injection using a MaestroTM in vivo imaging system (Cambridge Research & Instrumentation, Woburn, MA, USA). At 12 h postinjection, the mice were sacrificed. The tumor and major organs (liver, kidney, spleen, lung, and heart) were excised, followed by washing the surface with 0.9% NaCl for the ex vivo imaging of Cy5.5 NHS fluorescence. The resulting data can be used to identify, separate, and remove the contribution of auto fluorescence in analyzed images by the Carestream Molecular Imaging Software. The mice treated with 0.2 mL of the Cy5.5 NHS labeled MMC-PEG-CS-NPs or PEG-CS-NPs at Cy5.5-eq dose were used for comparison.

In Vivo Antitumor Efficacy. Kunming mice aged 4−5 weeks (clean class, 18−22 g) were supplied by Xiamen University Laboratory Animal Center and used in this study. Subcutaneous tumors were

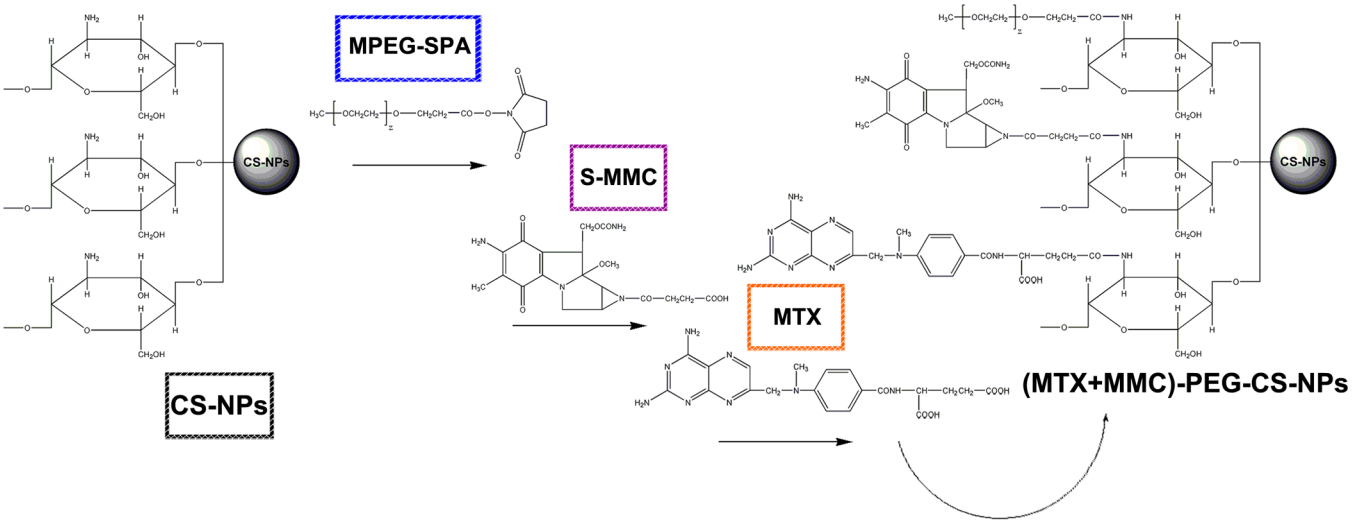

Figure 1. Synthetic scheme of the (MTX+MMC)-PEG-CS-NPs.

established in the mice by subcutaneous inoculation of 5×10^6 H_{22} cells in the right axillary region of the mice before the treatment. The H_{22} tumor bearing mice were randomly divided into 4 groups (10 mice per group): group 1 for 0.9% NaCl, group 2 for MTX+MMC injection, group 3 for MMC-PEG-CS-NPs, group 4 for (MTX +MMC)-PEG-CS-NPs. The mice were intravenously administrated at 4 mg/kg (MMC-eq dose) every 2 days for 2 times. Each mouse was earmarked and followed individually throughout the whole experiments. The body weight of mice was measured every day until the animals were terminated. The mice were terminated on day 7. The tumors were excised and then weighed. The tumor inhibition rate was calculated by the formula as previously reported.[45] The H_{22} tumor harvested from all 4 groups were fixed in 10% buffered formalin, embedded in paraffin, sectioned (5 μm), stained with hematoxylin and eosin (H&E), and examined using a digital microscopy system.

RESULTS AND DISCUSSION

Preparations of (MTX+MMC)-PEG-CS-NPs. The synthesized route of the (MTX+MMC)-PEG-CS-NPs were illustrated in Figure 1. We used a three-step procedure for the preparation of the (MTX+MMC)-PEG-CS-NPs based on the CS-NPs. First, the succinimidyl groups of MPEG-SPA were conjugated to the amino groups of the CS-NPs, as the PEG-CS-NPs with methoxy surface groups were ideal for drug delivery.[46] Subsequently, the succinic anhydride activated MMC (S-MMC) were coupled to the residual amino groups of the PEG-CS-NPs via carbodiimide chemistry.[35] Lastly, the MMC-PEG-CS-NPs were decorated with the Janus-like MTX via the interaction of the residual amino groups of MMC-PEG-CS-NPs and the γ-carboxyl groups within MTX.[47] The comparative FTIR spectra of PEG-CS-NPs, MMC-PEG-CS-NPs, and (MTX+MMC)-PEG-CS-NPs are shown in Figure 2. The PEG-CS-NPs showed an alkyl C−H stretching vibration at 2,886 cm^{-1} native to the structure of MPEG-SPA. The peak at 1,114 cm^{-1} also indicated the C−O−C stretching vibration, which was characteristic of repeated $-OCHH_2CH_2-$ units of the backbone of MPEG-SPA. Moreover, the PEG-CS-NPs also presented a strong peak at 1574 cm^{-1}, indicating the C═O stretching vibration owing to the successful PEGylation. After MMC modification, the absorption band at 1631 cm^{-1} was attributed to the C═C stretching vibration of S-MMC, and the absorption peak at 1499 cm^{-1} was assigned to the ring stretching vibrations of benzene. After further MTX modification, the absorption band at 1718 cm^{-1} indicated the

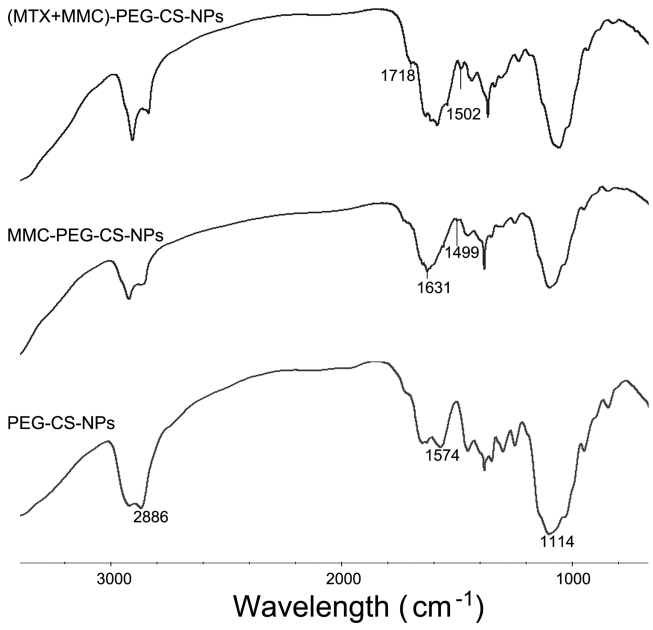

Figure 2. FTIR analysis of the PEG-CS-NPs, MMC-PEG-CS-NPs, and (MTX+MMC)-PEG-CS-NPs.

generation of the new C═O stretching vibration. In other words, the results suggested that the interaction between MMC-PEG-CS-NPs and MTX was at the level of a new amide bond.

As is reported, FA could be internalized into the cells through FA receptor-mediated endocytosis even when conjugated with a number of molecules.[48] Thus, the decoration of the targeting/cytotoxic MTX on the MMC loaded PEGylated CS-NPs could not only preserve its accessibility to the FA receptor site to preserve the targeting activity but also concomitantly avoid the premature drug release during circulation to reduce the side effects of chemotherapy.[29,49]

Particle Size, Particle Size Distribution, Zeta Potential, and Morphology. Knowledge of the particle size and zeta potential of the (MTX+MMC)-PEG-CS-NPs can help predict their fate at the cellular or animal level in vivo. Particle size of approximately 200 nm was suited for prolonged circulation because they can avoid liver uptake and rapid renal clearance.[5]

The incorporation of multiple drugs into the PEGylated CS-NPs was accompanied by the changes in particle size and zeta potential of the NPs (Table 1). After the modification of multiple drugs, the particle size increased from 210.5 to 215.0 nm, and the zeta potential increased from to 30.29 to 32.33 mV, which resulted from the multiple drugs tail with partial positive charge. The SEM images of the (MTX+MMC)-PEG-CS-NPs were presented in Figure 3, and the SEM images of their controlled sample are shown in Figure S1 in the Supporting Information. The well monodispersed NPs with a spherical shape (Figure 3C), a small particle size, a low PDI, a narrow particle size distribution, a high zeta potential, and an appreciable multiple drugs loading content (discussed below) implied that the (MTX+MMC)-PEG-CS-NPs were effective therapeutic drug delivery systems.

Table 1. Particle Size, PDI, and Zeta Potential of Various PEG-CS-NPs (n = 3)

	particle size (nm)	PDI	zeta potential (mV)
CS-NPs	192.2 ± 2.1	0.154 ± 0.017	41.30 ± 1.16
PEG-CS-NPs	210.5 ± 4.8	0.097 ± 0.006	30.29 ± 1.47
MMC-PEG-CS-NPs	213.6 ± 5.7	0.101 ± 0.014	31.87 ± 1.53
(MTX+MMC)-PEG-CS-NPs	215.0 ± 7.1	0.138 ± 0.019	32.33 ± 1.68

Drug Loading Content. CS polymer possessing peripheral amino groups provided us great opportunities for easy surface functionalization of the CS-NPs with various biological molecules. Additionally, CS could induce a proton-sponge effect to promote endo/lysosomal escape.[50] In our study, the carboxyl groups of the multiple drugs were conjugated to the residual amino groups of the PEGylated CS-NPs (see Figure 1). The MMC drug loading content of the (MTX+MMC)-PEG-CS-NPs was calculated as 37.54 ± 0.03%, and the MTX drug loading content of those was calculated as 10.40 ± 0.03%. On the encouraged result by the simple conjugation chemistry, the high MMC drug loading content of the PEGylated CS-NPs could improve the anticancer efficacy of MMC, meanwhile, the proper MTX drug loading content of those could favor the dual-acting role of Janus-like MTX.

In Vitro Enzymatic Drug Release. One of the advantages in the drug delivery systems is the controlled drug release. The drug release behavior of the (MTX+MMC)-PEG-CS-NPs in PBS could be divided into two phases. The initial burst release should be commonly attributed to the rapid diffusion of the NPs surface-associated drug, whereas the subsequent sustained release was likely due to the slow hydrolysis of peptide bonds.

To demonstrate that the majority of conjugated MTX and MMC can be released from the (MTX+MMC)-PEG-CS-NPs in the presence of crude proteases, a commercial proteolytic enzyme that can specifically hydrolyze the peptide bonds was added.[51,52] As shown in Figure 4, the (MTX+MMC)-PEG-CS-NPs presented a rapid release behavior with the addition of proteases and approximately 40% loaded MMC and 30% loaded MTX were released within 24 h. As a control, only no

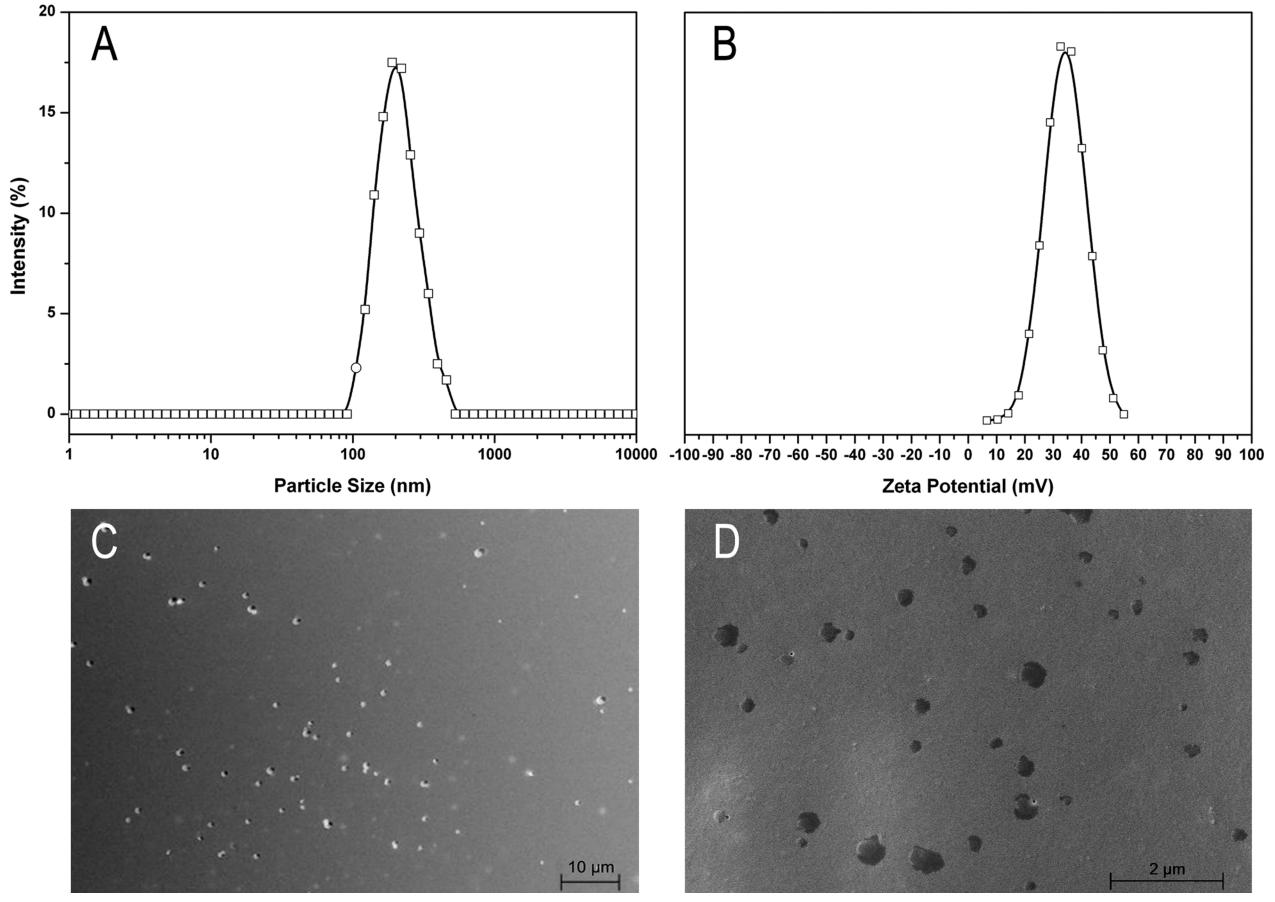

Figure 3. (A) Particle size distribution of the (MTX+MMC)-PEG-CS-NPs. (B) Zeta potential distribution of the (MTX+MMC)-PEG-CS-NPs. (C, D) SEM image of the (MTX+MMC)-PEG-CS-NPs.

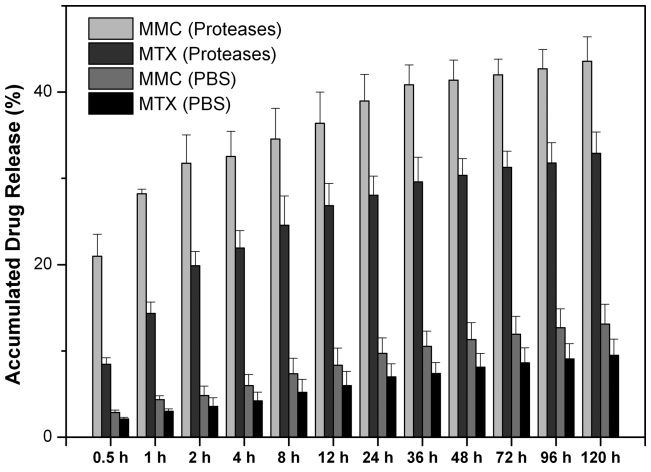

Figure 4. In vitro drug release behavior of the (MTX+MMC)-PEG-CS-NPs in PBS (pH 7.4) at physiological temperature (37 °C) with and without the addition of crude proteases.

more than 15% loaded MMC and 10% loaded MTX was accumulatively released within 120 h without the proteases. On the basis of the encouraging results, a majority of MTX and MMC were anticipated to be not prematurely released from the NPs in the circulation after intravenously administration. Moreover, we believed that once internalized inside target cells, the (MTX+MMC)-PEG-CS-NPs could also be preferentially hydrolyzed to release MMC and MTX by the endo/lysosomal proteases mediated selective cleavage of peptide bond as there were a number of types of proteases in tumor cells with various function.[53,54]

In Vitro Cellular Uptake. We investigated the cellular uptake of the FITC conjugated PEG-CS-NPs, MMC-PEG-CS-NPs, and (MTX+MMC)-PEG-CS-NPs by HeLa cells using CLSM. To better compare cell internalization among the various PEG-CS-NPs formulation, the images were taken by harmonizing the parameters such as laser power, sensitivity, offset, and gain constant during the cell imaging procedure.[14] Figure 5 showed that the similar fluorescence intensity was observed in HeLa cells treated with the FITC conjugated PEG-CS-NPs compared to those treated with the FITC conjugated MMC-PEG-CS-NPs. It was revealed that the MMC modification did not alter the cellular uptake character of the PEG-CS-NPs significantly. However, when HeLa cells were treated with the FITC conjugated (MTX+MMC)-PEG-CS-NPs, the fluorescence intensity was significantly stronger. The result indicated that the further MTX modification improves the cellular uptake efficacy. These results can be explained by their distinct uptake mechanisms.[55] The PEG-CS-NPs and MMC-PEG-CS-NPs with the particle size of approximately 200 nm and the positive surface charge may be absorbed by the cells through clathrin- or caveolae-mediated endocytosis,[55] while the (MTX+MMC)-PEG-CS-NPs could be internalized into the cells by FA receptor-mediated endocytosis.[29,30]

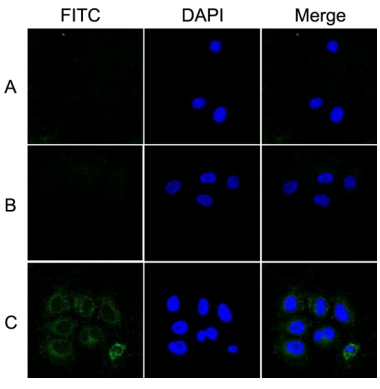

Figure 5. In vitro cellular uptake of the (MTX+MMC)-PEG-CS-NPs. HeLa cells were treated with the (A) FITC conjugated PEG-CS-NPs; (B) FITC conjugated MMC-PEG-CS-NPs; and (C) FITC conjugated (MTX+MMC)-PEG-CS-NPs for 12 h and then observed by CLSM. The nuclei was stained by DAPI (blue).

More notably, the green circles around HeLa cells in merge image of Figure 5C indicated certain FITC conjugated (MTX+MMC)-PEG-CS-NPs bound on the surface of the cells. This different cell attachment and internalization also attributed to different endocytosis mechanisms.[56] The (MTX+MMC)-PEG-CS-NPs could be transported into the cells by a specific ligand−receptor interaction other than simply nonspecific absorption depending on the particle size as well as surface charge. The high selective efficiency made those NPs as promising candidates for therapeutic drug delivery with expected targeting effect and reducing side effect.[57]

In Vitro Cell Viability Tests. MTX and MMC were used as a pair to demonstrate the effect of codelivery of multiple anticancer drugs in the same drug carriers. HeLa cells were treated with the (MTX+MMC)-PEG-CS-NPs for three different times (24, 48 and 72 h). On the one hand, the PEG-CS-NPs and MMC-PEG-CS-NPs were used for comparison to test the efficacy of simultaneous multiple drug delivery. On the other hand, the free MTX+MMC were used for comparison to test the efficacy of the drug carriers. The cell viability was evaluated by MTT assay (Figure 6).

No significant adverse effect against HeLa cells was demonstrated in the PEG-CS-NPs, indicating the biocompatible feature of the drug carriers. Delivering multiple MMC and MTX drugs by the PEG-CS-NPs with the time-dependent cytotoxicity significantly reduced cell viability compared to delivering a single MMC drug (Figure 6A and 6B). It was suggested that the synergistic anticancer effects of the (MTX+MMC)-PEG-CS-NPs might result from the combination of individual anticancer mechanisms for each drug. As mentioned above, MMC can be bound to DNA by intercalation and motivated a series of biochemical events inducing apoptosis/death in cancer cells, and MTX can be bound with DHFR, thereby inducing the inhibition of nucleic acid biosynthsis and subsequent cell death. Synthetically considering the other factor that the targeting effect of Janus-like MTX played a role in the enhanced cytotoxic effects (see Figure 5), treating cancer with MMC and Janus-like MTX might achieve the synergistic effects to accelerate cancer apoptosis/death for in vivo application.

Besides, the (MTX+MMC)-PEG-CS-NPs induced a low cytotoxicity on HeLa cells compared to the free MTX+MMC at an equivalent MTX or MMC concentration (Figure 6A), which was most probably because of the prolonged drug release from the multiple drugs-loaded NPs (see Figure 4), which was also consistent with the previous report.[58] On the contrary, under in vitro conditions, the free drugs can be rapidly transported into cells by passive diffuse owing to the driving force of a pH and concentration gradient and instantaneously inhibiting the cell growth without the drug release process.[15,59] It was also found that the (MTX+MMC)-PEG-CS-NPs (20 μg/mL of MMC) induced the enhanced cytotoxicity for a long incubation time (48 and 72 h), while the mixtures of MTX and MMC exhibited

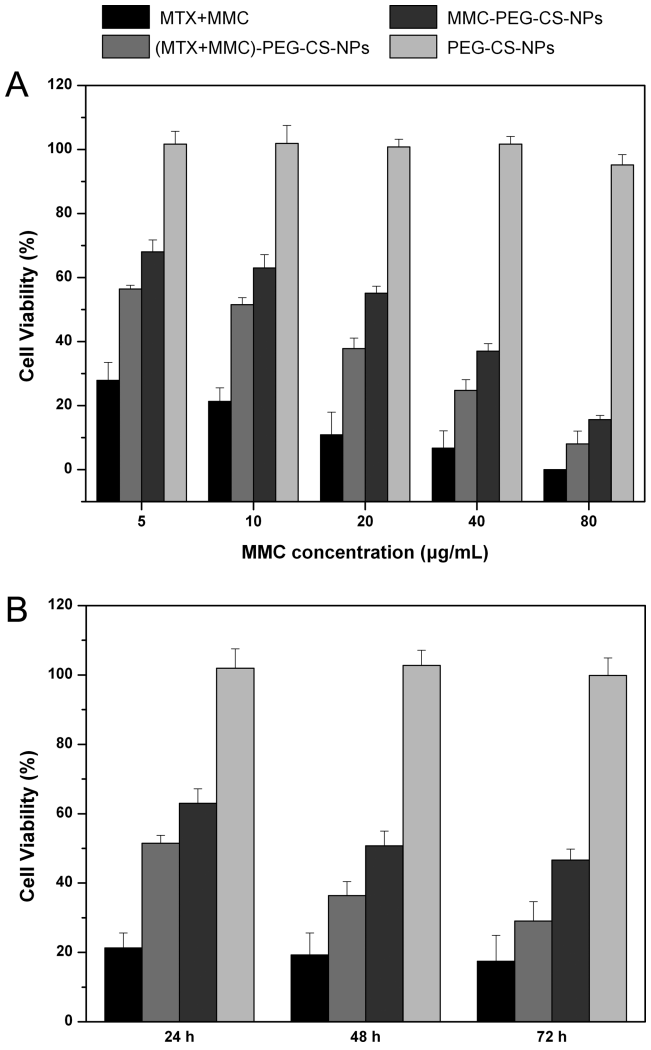

Figure 6. (A) In vitro cell viability of different formulations (PEG-CS-NPs, MMC-PEG-CS-NPs, (MTX+MMC)-PEG-CS-NPs, MTX +MMC) on HeLa cells at different MMC drug concentration. The drug concentration ratio of MMC to MTX was 3.6:1 in the (MTX +MMC)-PEG-CS-NPs or free MTX+MMC. (B) In vitro cell viability of different formulations on HeLa cells at an equivalent MMC concentration (10 μg/mL) for different incubation times.

no significant difference in cytotoxicity at different incubation times (Figure 6B), further suggesting that such delayed drug release behavior of the (MTX+MMC)-PEG-CS-NPs might result in the progressive increase of intracellular drug level for cell apoptosis/death.

Furthermore, taking into account of the sustained drug release characteristic of the NPs, some reported studies have described that the mortality of cells treated with the NPs should be corrected by the accumulated drug release.[15,60] The equation of correction is as follows:

$$\text{modified mortality} = (\text{measured mortality}/\text{accumulated drug release}) \times 2$$

In this study, 31.28% of MTX and 41.98% of MMC was released from the (MTX+MMC)-PEG-CS-NPs after 72 h in PBS with proteases (see Figure 4). In the case of the free MTX +MMC, almost 100% of multiple drugs were released out after the same time in the same media. The modified mortality of the (MTX+MMC)-PEG-CS-NPs in HeLa cells at equivalent MTX and MMC concentration after 72 h incubation were 3.19 times higher than that of the free MTX+MMC after correction through the drug release, indicating that the multiple drugs loaded NPs could induce the cancer cell apoptosis/death more effectively compared to the free multiple drugs. More noticeably, the targeting efficacy of the NPs would increase the tumor accumulation of the more amounts of drugs loaded within the NPs during circulation in vivo, which was confirmed by in vivo tumor targeting imaging (discussed below).

In/Ex Vivo Tumor Targeted Imaging. To evaluate the biodistribution and tumor targeting efficiency of various PEG-CS-NPs, Cy5.5 NHS as a near-infrared fluorescent dye was used to conjugate to various PEG-CS-NPs, and a noninvasive near-infrared optical imaging technology was used in this study. The tumor model was established by inoculating H_{22} cells in the right axillary region of BALB/c nude mice.

In vivo fluorescent images were taken at different time points after intravenously administration. Figure 7A showed the real-time images of the Cy5.5 NHS conjugated PEG-CS-NPs, MMC-PEG-CS-NPs, and (MTX+MMC)-PEG-CS-NPs in the tumor-bearing mice. In vivo fluorescent images showed that Cy5.5 NHS conjugated (MTX+MMC)-PEG-CS-NPs were clearly accumulated in the tumor, and the fluorescent signal at 1 h reached the highest. Then the fluorescent signal gradually became weaker as the time elapsed. However, the strong fluorescent signal still maintained to 6 h. On the contrary, the less fluorescent signal of the Cy5.5 NHS conjugated MMC-PEG-CS-NPs and PEG-CS-NPs in the tumor were observed.

As shown in Figure 7B which gave the ex vivo image, the tumor of mice treated with the Cy5.5 NHS conjugated (MTX +MMC)-PEG-CS-NPs at 6 h after injection showed a significantly stronger fluorescent signal than that treated with the Cy5.5 NHS conjugated MMC-PEG-CS-NPs or PEG-CS-NPs. These results further confirmed that the introduction of MTX molecule could assist the targeting effect of the NPs to the tumor. The high accumulation of the Cy5.5 NHS conjugated MMC-PEG-CS-NPs or PEG-CS-NPs was observed in the RES organs such as liver, possibly caused by the clearance of the RES. Most importantly, compared to the Cy5.5 NHS conjugated MMC-PEG-CS-NPs or PEG-CS-NPs group, the Cy5.5 NHS conjugated (MTX+MMC)-PEG-CS-NPs group showed the decreased accumulation of the fluorescence in the major organs but the increased accumulation of that in the tumor, indicating the less RES uptake and higher tumor accumulation of the Cy5.5 NHS conjugated (MTX+MMC)-PEG-CS-NPs. All results suggested that the (MTX+MMC)-PEG-CS-NPs possessed superior tumor targeting efficiency for tumor-specific drug delivery.

In Vivo Antitumor Effects. To examine in vivo antitumor effects, we treated Kunming mice bearing the H_{22} tumor with 0.9% NaCl, MMC-PEG-CS-NPs, (MTX+MMC)-PEG-CS-NPs, and free MTX+MMC. All the mice were alive during the experimental period (Table 2). As shown in Figure 8A and Table 1, compared to the control group, the tumor weights in three treatment groups were significantly smaller after a schedule of multiple doses, indicating the effective tumor inhibition efficacy. It indicated that the (MTX+MMC)-PEG-CS-NPs had superior anticancer efficacy compared with the MMC-PEG-CS-NPs ($p < 0.05$), further proving that the MTX modification increased the anticancer efficacy because of the higher accumulation in the tumor site (see Figure 7) and the facilitated cellular uptake by the tumor cells (see Figure 5).

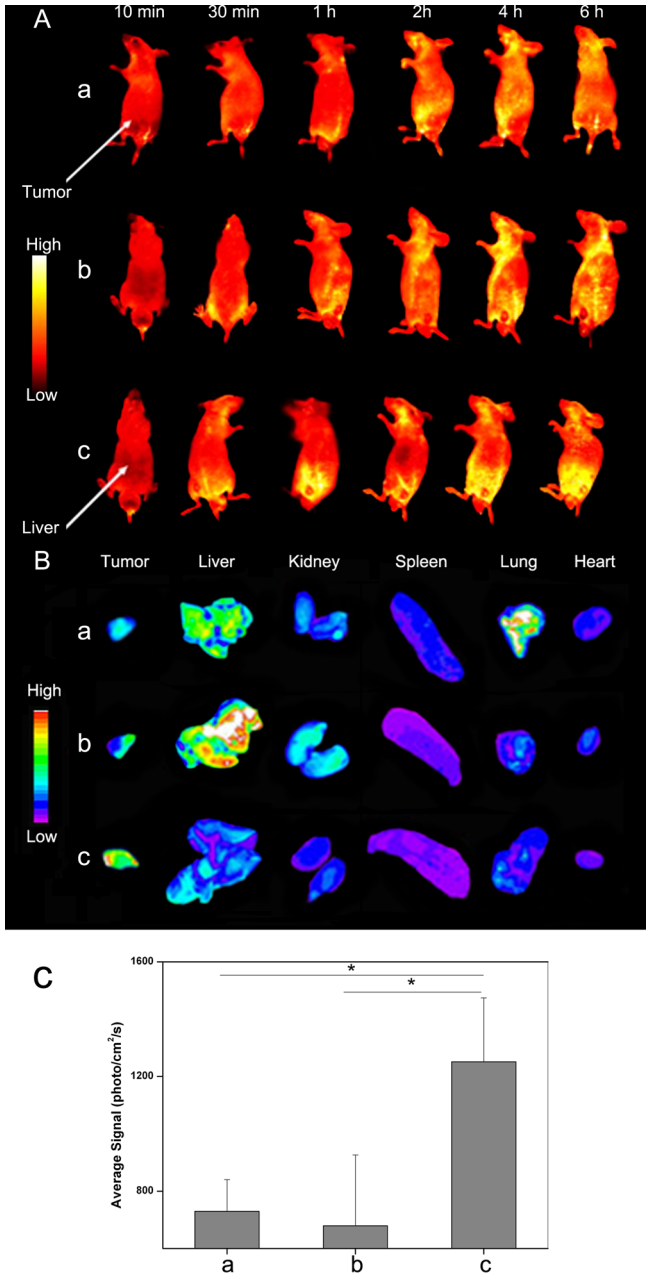

Figure 7. In vivo tumor targeted imaging of the (MTX+MMC)-PEG-CS-NPs in the BALB/c mice bearing H_{22} tumor. (a) Cy5.5 NHS conjugated PEG-CS-NPs, (b) Cy5.5 NHS conjugated MMC-PEG-CS-NPs, (c) Cy5.5 NHS conjugated (MTX+MMC)-PEG-CS-NPs. (A) In vivo fluorescence imaging of H_{22} tumor-bearing mice treated with different formulations at different time points. (B) Ex vivo fluorescence imaging of main organs and tumor excised from the tumor-bearing mice at 6 h postinjection. (C) Quantitative tumor target characteristics of different formulations (mean ± SD, n = 3). * $P < 0.05$.

Notably, although the cytotoxicity of the free MTX+MMC was higher than that of the (MTX+MMC)-PEG-CS-NPs in vitro, the (MTX+MMC)-PEG-CS-NPs exhibited the enhanced tumor inhibition against the H_{22} tumor. The result was probably due to the EPR effect, extended blood circulation time, receptor-mediated targeting, and sustained drug release of the (MTX+MMC)-PEG-CS-NPs.

Additional evidence of enhanced anticancer effects of the (MTX+MMC)-PEG-CS-NPs was obtained by H&E staining

Table 2. Tumor Inhibition Effect of Different Formulations (n = 7)

	tumor weight				
formulation	mean	SD	survival mice at 7th day	tumor inhibition rate %	P
0.9% NaCl	0.693	0.054	7		
MMC-PEG-CS-NPs	0.500	0.040	7	27.8	<0.05
(MTX+MMC)-PEG-CS-NPs	0.283	0.039	7	59.2	<0.05
MTX+MMC	0.636	0.033	7	8.24	<0.05

(Figure 8C). Compared to the control, some observed necrotic regions distributed in the tumor section of the free MTX +MMC. More notably, the (MTX+MMC)-PEG-CS-NPs displayed the majority of necrosis, further indicating their outstanding anticancer efficacy. These results suggested that the (MTX+MMC)-PEG-CS-NPs were significantly more effective in inducing the cell apoptosis/death and reducing the cell proliferation than the combination of the free multiple drugs, which might be explained by the NPs size effect/the targeting effect-mediated more uptake and greater accumulation in tumor cells. Most importantly, the (MTX+MMC)-PEG-CS-NPs, as successful nanoscaled codelivery systems, could simultaneously deliver MTX and MMC to the tumor site, which would contribute to more efficiently synergistic anticancer effects.

For any drug delivery system, the systemic toxicity should be considered to ensure safety even if the system has an outstanding therapeutic effect. In this study, the potential toxicity of different formulations was determined by monitoring animal behavior and weight loss. As shown in Figure 8B, compared to the control group, the free MTX+MMC group yielded pronounced body weight loss ($p < 0.05$), while the mice was listlessness/laziness after intravenous administration. The result was indicative of the undesirable side effects of chemotherapy. On the contrary, no undesirable side effects, such as decreased body weight and remarkable change in activity were shown in the (MTX+MMC)-PEG-CS-NPs group. Overall, these results suggested that the (MTX+MMC)-PEG-CS-NPs were expected to be effective in maximizing therapeutic effects of MMC with minimizing its toxicity to synergize the therapeutic index and greatly improve the patient's quality of life.

CONCLUSION

In this study, we prepared the Janus-like MTX targeted and MMC loaded PEGylated CS-NPs. The (MTX+MMC)-PEG-CS-NPs showed a nanoscaled particle size/narrow size distribution, high MMC drug loading content/proper MTX drug loading content, and sustained multiple drug release. Based on the FA receptor-mediated endocytosis as well as EPR effects, the (MTX+MMC)-PEG-CS-NPs could be efficiently taken up by cancer cells and subsequently assist the drugs targeting to the tumor. Moreover, the (MTX+MMC)-PEG-CS-NPs demonstrated the greater tumor growth inhibition in vivo with the reduced toxicity. Therefore, the (MTX+MMC)-PEG-CS-NPs can be considered as promising targeted codelivery systems for combination cancer chemotherapy.

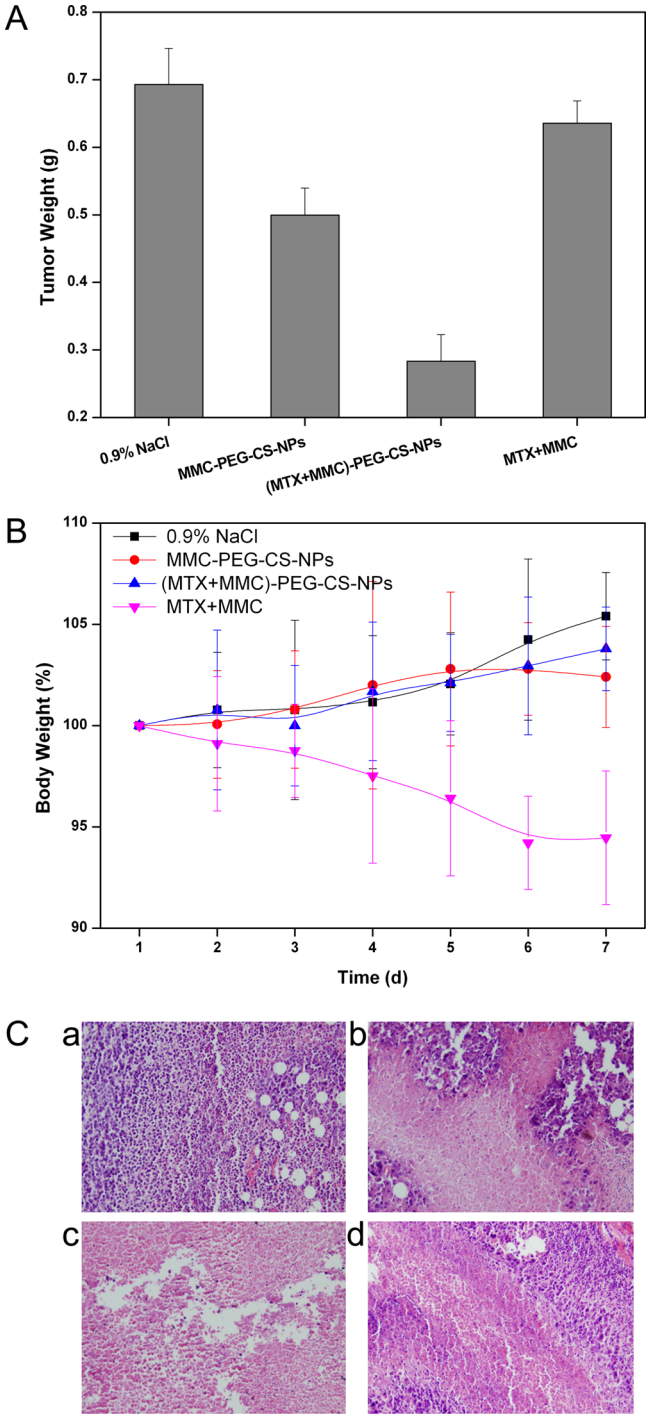

Figure 8. In vivo antitumor effects of different formulations (0.9% NaCl, MMC-PEG-CS-NPs, (MTX+MMC)-PEG-CS-NPs, MTX +MMC) in Kunming mice bearing the H_{22} tumor. (A) Quantitative results of tumor weight excised from the tumor-bearing mice sacrificed on day 7. (B) Body weight changes of the tumor-bearing mice during the treatment. (C) Histological section of the tumor of the mice after the treatment with (a) 0.9% NaCl, (b) MMC-PEG-CS-NPs, (c) (MTX+MMC)-PEG-CS-NPs, (d) MTX+MMC.

■ ASSOCIATED CONTENT

Ⓢ Supporting Information

Figure S1. This material is available free of charge via the Internet at http://pubs.acs.org.

■ AUTHOR INFORMATION

Corresponding Authors

*E-mail: Houzhenqing@xmu.edu.cn.
*E-mail: Zhangqiq@126.com.

Author Contributions

⊥Authors M.J. and Y.L. contributed equally.

Notes

The authors declare no competing financial interest.

■ ACKNOWLEDGMENTS

This study was supported by the Natural Science Foundation of China (Grant No. 31271071) and the major research plan of the National Natural Science Foundation (Grant No. 91323104)

■ ABBREVIATIONS USED

MMC = mitomycin C
S-MMC = succinic anhydride activated MMC
MTX = methotrexate
FTIR = Fourier transform infrared spectroscopy
DLS = dynamic light scattering
SLS = static light scattering
PDI = polydispersity index
SEM = scanning electron microscopy
CLSM = confocal laser scanning microscopy
HPLC = high-performance liquid chromatography

■ REFERENCES

(1) Jemal, A.; Bray, F.; Center, M. M.; Ferlay, J.; Ward, E.; Forman, D. Global Cancer Statistics. *Ca-Cancer J. Clin.* **2011**, *61*, 69−90.
(2) Weeks, J. C.; Catalano, P. J.; Cronin, A.; Finkelman, M. D.; Mack, J. W.; Keating, N. L.; Schrag, D. Patients' Expectations About Effects of Chemotherapy for Advanced Cancer. *N. Engl. J. Med.* **2012**, *367*, 1616−1625.
(3) Hubbell, J. A.; Chilkoti, A. Nanomaterials for Drug Delivery. *Science* **2012**, *337*, 303−305.
(4) Peer, D.; Karp, J. M.; Hong, S.; Farokhzad, O. C.; Margalit, R.; Langer, R. Nanocarriers as an Emerging Platform for Cancer Therapy. *Nat. Nanotechnol.* **2007**, *2*, 751−760.
(5) Petros, R. A.; DeSimone, J. M. Strategies in the Design of Nanoparticles for Therapeutic Applications. *Nat. Rev. Drug Discovery* **2010**, *9*, 615−627.
(6) Greco, F.; Vicent, M. J. Combination Therapy: Opportunities and Challenges for Polymer-Drug Conjugates as Anticancer Nanomedicines. *Adv. Drug Delivery Rev.* **2009**, *61*, 1203−1213.
(7) Parhi, P.; Mohanty, C.; Sahoo, S. K. Nanotechnology-Based Combinational Drug Delivery: An Emerging Approach for Cancer Therapy. *Drug Discovery Today* **2012**, *17*, 1044−1052.
(8) Ma, L.; Kohli, M.; Smith, A. Nanoparticles for Combination Drug Therapy. *ACS Nano* **2013**, *7*, 9518−9525.
(9) Woodcock, J.; Griffin, J. P.; Behrman, R. E. Development of Novel Combination Therapies. *N. Engl. J. Med.* **2011**, *364*, 985−987.
(10) Kaelin, W. G., Jr. The Concept of Synthetic Lethality in the Context of Anticancer Therapy. *Nat. Rev. Cancer* **2005**, *5*, 689−698.
(11) Lehar, J.; Krueger, A. S.; Avery, W.; Heilbut, A. M.; Johansen, L. M.; Price, E. R.; Rickles, R. J.; Short, G. F., 3rd; Staunton, J. E.; Jin, X.; Lee, M. S.; Zimmermann, G. R.; Borisy, A. A. Synergistic Drug Combinations Tend to Improve Therapeutically Relevant Selectivity. *Nat. Biotechnol.* **2009**, *27*, 659−666.
(12) Mitragotri, S. Synergistic Effect of Enhancers for Transdermal Drug Delivery. *Pharm. Res.* **2000**, *17*, 1354−1359.
(13) Walsh, C. Molecular Mechanisms That Confer Antibacterial Drug Resistance. *Nature* **2000**, *406*, 775−781.
(14) Wang, H.; Zhao, Y.; Wu, Y.; Hu, Y. L.; Nan, K.; Nie, G.; Chen, H. Enhanced Anti-Tumor Efficacy by Co-Delivery of Doxorubicin and

Paclitaxel with Amphiphilic Methoxy Peg-Plga Copolymer Nanoparticles. *Biomaterials* **2011**, *32*, 8281−8290.
(15) Yao, J.; Zhang, L.; Zhou, J.; Liu, H.; Zhang, Q. Efficient Simultaneous Tumor Targeting Delivery of All-Trans Retinoid Acid and Paclitaxel Based on Hyaluronic Acid-Based Multifunctional Nanocarrier. *Mol. Pharmacol.* **2013**, *10*, 1080−1091.
(16) Duan, X.; Xiao, J.; Yin, Q.; Zhang, Z.; Yu, H.; Mao, S.; Li, Y. Smart Ph-Sensitive and Temporal-Controlled Polymeric Micelles for Effective Combination Therapy of Doxorubicin and Disulfiram. *ACS Nano* **2013**, *7*, 5858−5869.
(17) Shanmugam, V.; Chien, Y. H.; Cheng, Y. S.; Liu, T. Y.; Huang, C. C.; Su, C. H.; Chen, Y. S.; Kumar, U.; Hsu, H. F.; Yeh, C. S. Oligonucleotides-Assembled Au Nanorod-Assisted Cancer Photothermal Ablation and Combination Chemotherapy with Targeted Dual-Drug Delivery of Doxorubicin and Cisplatin Prodrug. *ACS Appl. Mater. Interfaces* **2014**, *6*, 4382−4393.
(18) Fang, J. H.; Lai, Y. H.; Chiu, T. L.; Chen, Y. Y.; Hu, S. H.; Chen, S. Y. Magnetic Core-Shell Nanocapsules with Dual-Targeting Capabilities and Co-Delivery of Multiple Drugs to Treat Brain Gliomas. *Adv. Healthcare Mater.* **2014**, DOI: 10.1002/adhm.201300598.
(19) Aryal, S.; Hu, C. M.; Zhang, L. Polymeric Nanoparticles with Precise Ratiometric Control over Drug Loading for Combination Therapy. *Mol. Pharmaceutics* **2011**, *8*, 1401−1407.
(20) Bradner, W. T. Mitomycin C: A Clinical Update. *Cancer Treat. Rev.* **2001**, *27*, 35−50.
(21) Jolivet, J.; Cowan, K. H.; Curt, G. A.; Clendeninn, N. J.; Chabner, B. A. The Pharmacology and Clinical Use of Methotrexate. *N. Engl. J. Med.* **1983**, *309*, 1094−1104.
(22) Iyer, V. N.; Szybalski, W. Mitomycins and Porfiromycin: Chemical Mechanism of Activation and Cross-Linking of DNA. *Science* **1964**, *145*, 55−58.
(23) Matthews, D. A.; Alden, R. A.; Bolin, J. T.; Freer, S. T.; Hamlin, R.; Xuong, N.; Kraut, J.; Poe, M.; Williams, M.; Hoogsteen, K. Dihydrofolate Reductase: X-Ray Structure of the Binary Complex with Methotrexate. *Science* **1977**, *197*, 452−455.
(24) Roberts, G. C.; Feeney, J.; Birdsall, B.; Charlton, P.; Young, D. Methotrexate Binding to Dihydrofolate Reductase. *Nature* **1980**, *286*, 309.
(25) Hou, Z.; Li, Y.; Huang, Y.; Zhou, C.; Lin, J.; Wang, Y.; Cui, F.; Zhou, S.; Jia, M.; Ye, S.; Zhang, Q. Phytosomes Loaded with Mitomycin C-Soybean Phosphatidylcholine Complex Developed for Drug Delivery. *Mol. Pharmacol.* **2013**, *10*, 90−101.
(26) Tomasz, M.; Lipman, R.; Chowdary, D.; Pawlak, J.; Verdine, G. L.; Nakanishi, K. Isolation and Structure of a Covalent Cross-Link Adduct between Mitomycin C and DNA. *Science* **1987**, *235*, 1204−1208.
(27) Rajagopalan, P. T.; Zhang, Z.; McCourt, L.; Dwyer, M.; Benkovic, S. J.; Hammes, G. G. Interaction of Dihydrofolate Reductase with Methotrexate: Ensemble and Single-Molecule Kinetics. *Proc. Natl. Acad. Sci. U. S. A.* **2002**, *99*, 13481−13486.
(28) Tanabe, M.; Ito, Y.; Tokudome, N.; Sugihara, T.; Miura, H.; Takahashi, S.; Seto, Y.; Iwase, T.; Hatake, K. Possible Use of Combination Chemotherapy with Mitomycin C and Methotrexate for Metastatic Breast Cancer Pretreated with Anthracycline and Taxanes. *Breast Cancer* **2009**, *16*, 301−306.
(29) Rosenholm, J. M.; Peuhu, E.; Bate-Eya, L. T.; Eriksson, J. E.; Sahlgren, C.; Linden, M. Cancer-Cell-Specific Induction of Apoptosis Using Mesoporous Silica Nanoparticles as Drug-Delivery Vectors. *Small* **2010**, *6*, 1234−1241.
(30) Thomas, T. P.; Huang, B.; Choi, S. K.; Silpe, J. E.; Kotlyar, A.; Desai, A. M.; Zong, H.; Gam, J.; Joice, M.; Baker, J. R., Jr. Polyvalent Dendrimer-Methotrexate as a Folate Receptor-Targeted Cancer Therapeutic. *Mol. Pharmaceutics* **2012**, *9*, 2669−2676.
(31) Rijnboutt, S.; Jansen, G.; Posthuma, G.; Hynes, J. B.; Schornagel, J. H.; Strous, G. J. Endocytosis of Gpi-Linked Membrane Folate Receptor-Alpha. *J. Cell Biol.* **1996**, *132*, 35−47.
(32) Qiu, A.; Jansen, M.; Sakaris, A.; Min, S. H.; Chattopadhyay, S.; Tsai, E.; Sandoval, C.; Zhao, R.; Akabas, M. H.; Goldman, I. D. Identification of an Intestinal Folate Transporter and the Molecular Basis for Hereditary Folate Malabsorption. *Cell* **2006**, *127*, 917−928.
(33) Wosikowski, K.; Biedermann, E.; Rattel, B.; Breiter, N.; Jank, P.; Loser, R.; Jansen, G.; Peters, G. J. In Vitro and in Vivo Antitumor Activity of Methotrexate Conjugated to Human Serum Albumin in Human Cancer Cells. *Clin. Cancer Res.* **2003**, *9*, 1917−1926.
(34) Dopieralski, P.; Ribas-Arino, J.; Anjukandi, P.; Krupicka, M.; Kiss, J.; Marx, D. The Janus-Faced Role of External Forces in Mechanochemical Disulfide Bond Cleavage. *Nat. Chem.* **2013**, *5*, 685−691.
(35) Kuan, S. L.; Ng, D. Y. W.; Wu, Y.; Förtsch, C.; Barth, H.; Doroshenko, M.; Koynov, K.; Meier, C.; Weil, T. Ph Responsive Janus-Like Supramolecular Fusion Proteins for Functional Protein Delivery. *J. Am. Chem. Soc.* **2013**, *135*, 17254−17257.
(36) Wilson, S. B.; Delovitch, T. L. Janus-Like Role of Regulatory Inkt Cells in Autoimmune Disease and Tumour Immunity. *Nat. Rev. Immunol.* **2003**, *3*, 211−222.
(37) Amidi, M.; Mastrobattista, E.; Jiskoot, W.; Hennink, W. E. Chitosan-Based Delivery Systems for Protein Therapeutics and Antigens. *Adv. Drug Delivery Rev.* **2010**, *62*, 59−82.
(38) Garcia-Fuentes, M.; Alonso, M. J. Chitosan-Based Drug Nanocarriers: Where Do We Stand? *J. Controlled Release* **2012**, *161*, 496−504.
(39) Mao, S.; Sun, W.; Kissel, T. Chitosan-Based Formulations for Delivery of DNA and Sirna. *Adv. Drug Delivery Rev.* **2010**, *62*, 12−27.
(40) Agnihotri, S. A.; Mallikarjuna, N. N.; Aminabhavi, T. M. Recent Advances on Chitosan-Based Micro- and Nanoparticles in Drug Delivery. *J. Controlled Release* **2004**, *100*, 5−28.
(41) Hou, Z.; Zhan, C.; Jiang, Q.; Hu, Q.; Li, L.; Chang, D.; Yang, X.; Wang, Y.; Li, Y.; Ye, S.; Xie, L.; Yi, Y.; Zhang, Q. Both Fa- and Mpeg-Conjugated Chitosan Nanoparticles for Targeted Cellular Uptake and Enhanced Tumor Tissue Distribution. *Nanoscale Res. Lett.* **2011**, *6*, 563−573.
(42) Chen, J.; Huang, L.; Lai, H.; Lu, C.; Fang, M.; Zhang, Q.; Luo, X. Methotrexate-Loaded Pegylated Chitosan Nanoparticles: Synthesis, Characterization, and in Vitro and in Vivo Antitumoral Activity. *Mol. Pharmaceutics* **2013**, DOI: 10.1021/mp400269z.
(43) Moghimi, S. M.; Hunter, A. C.; Murray, J. C. Long-Circulating and Target-Specific Nanoparticles: Theory to Practice. *Pharmacol. Rev.* **2001**, *53*, 283−318.
(44) Li, M.; Song, W.; Tang, Z.; Lv, S.; Lin, L.; Sun, H.; Li, Q.; Yang, Y.; Hong, H.; Chen, X. Nanoscaled Poly(L-Glutamic Acid)/Doxorubicin-Amphiphile Complex as Ph-Responsive Drug Delivery System for Effective Treatment of Nonsmall Cell Lung Cancer. *ACS Appl. Mater. Interfaces* **2013**, *5*, 1781−1792.
(45) Jin, E.; Zhang, B.; Sun, X.; Zhou, Z.; Ma, X.; Sun, Q.; Tang, J.; Shen, Y.; Van Kirk, E.; Murdoch, W. J.; Radosz, M. Acid-Active Cell-Penetrating Peptides for in Vivo Tumor-Targeted Drug Delivery. *J. Am. Chem. Soc.* **2013**, *135*, 933−940.
(46) Salvador-Morales, C.; Zhang, L.; Langer, R.; Farokhzad, O. C. Immunocompatibility Properties of Lipid-Polymer Hybrid Nanoparticles with Heterogeneous Surface Functional Groups. *Biomaterials* **2009**, *30*, 2231−2240.
(47) Kohler, N.; Sun, C.; Fichtenholtz, A.; Gunn, J.; Fang, C.; Zhang, M. Methotrexate-Immobilized Poly(Ethylene Glycol) Magnetic Nanoparticles for Mr Imaging and Drug Delivery. *Small* **2006**, *2*, 785−792.
(48) Low, P. S.; Henne, W. A.; Doorneweerd, D. D. Discovery and Development of Folic-Acid-Based Receptor Targeting for Imaging and Therapy of Cancer and Inflammatory Diseases. *Acc. Chem. Res.* **2008**, *41*, 120−129.
(49) Cheng, Z.; Al Zaki, A.; Hui, J. Z.; Muzykantov, V. R.; Tsourkas, A. Multifunctional Nanoparticles: Cost Versus Benefit of Adding Targeting and Imaging Capabilities. *Science* **2012**, *338*, 903−910.
(50) Richard, I.; Thibault, M.; De Crescenzo, G.; Buschmann, M. D.; Lavertu, M. Ionization Behavior of Chitosan and Chitosan-DNA Polyplexes Indicate That Chitosan Has a Similar Capability to Induce a Proton-Sponge Effect as Pei. *Biomacromolecules* **2013**, *14*, 1732−1740.

(51) Romberg, B.; Hennink, W. E.; Storm, G. Sheddable Coatings for Long-Circulating Nanoparticles. *Pharm. Res.* **2008**, *25*, 55−71.
(52) Poole, A. R.; Tiltman, K. J.; Recklies, A. D.; Stoker, T. A. M. Differences in Secretion of the Proteinase Cathepsin B at the Edges of Human Breast Carcinomas and Fibroadenomas. *Nature* **1978**, *273*, 545−547.
(53) Hedstrom, L. Serine Protease Mechanism and Specificity. *Chem. Rev.* **2002**, *102*, 4501−4524.
(54) Southan, C. A Genomic Perspective on Human Proteases as Drug Targets. *Drug Discovery Today* **2001**, *6*, 681−688.
(55) Rejman, J.; Oberle, V.; Zuhorn, I. S.; Hoekstra, D. Size-Dependent Internalization of Particles Via the Pathways of Clathrin- and Caveolae-Mediated Endocytosis. *Biochem. J.* **2004**, *377*, 159−169.
(56) Kievit, F. M.; Zhang, M. Cancer Nanotheranostics: Improving Imaging and Therapy by Targeted Delivery across Biological Barriers. *Adv. Mater.* **2011**, *23*, H217−247.
(57) Zhou, D.; Zhang, G.; Gan, Z. C(Rgdfk) Decorated Micellar Drug Delivery System for Intravesical Instilled Chemotherapy of Superficial Bladder Cancer. *J. Controlled Release* **2013**, *169*, 204−210.
(58) Min, K. H.; Park, K.; Kim, Y.-S.; Bae, S. M.; Lee, S.; Jo, H. G.; Park, R.-W.; Kim, I.-S.; Jeong, S. Y.; Kim, K.; Kwon, I. C. Hydrophobically Modified Glycol Chitosan Nanoparticles-Encapsulated Camptothecin Enhance the Drug Stability and Tumor Targeting in Cancer Therapy. *J. Controlled Release* **2008**, *127*, 208−218.
(59) Yue, J.; Liu, S.; Wang, R.; Hu, X.; Xie, Z.; Huang, Y.; Jing, X. Transferrin-Conjugated Micelles: Enhanced Accumulation and Antitumor Effect for Transferrin-Receptor-Overexpressing Cancer Models. *Mol. Pharmaceutics* **2012**, *9*, 1919−1931.
(60) Dong, Y.; Feng, S. S. In Vitro and in Vivo Evaluation of Methoxy Polyethylene Glycol-Polylactide (Mpeg-Pla) Nanoparticles for Small-Molecule Drug Chemotherapy. *Biomaterials* **2007**, *28*, 4154−4160.